Supplemental text and figures for:

NKCC1-Dependent GABAergic Excitation Drives Synaptic Network Maturation During Early Hippocampal Development

by

Carsten K. Pfeffer, Valentin Stein, Damien J. Keating, Hannes Maier, Ilka Rinke, York Rudhard, Moritz Hentschke, Gabriele Rune, Thomas J. Jentsch and Christian A. Hübner

Supplementary Table 1:

Sequence 5´ > 3´	Gene
CATGCCAGCAAAGCACCAT	AE3 forward
AGAAGTGCAATGCAGCCCA	AE3 reverse
CCGCCAAACCCAATGTGAT	Arc forward
TGCTTGGACACTTCGGTCAAC	Arc reverse
GCTGAAGGCGTGCGAGTATTA	BDNF ex4 forward
GAGTCTTTGGTGGCCGATATG	BDNF ex4 reverse
GGAATGGTGAAGACCGTGTCA	cFOS forward
CCCTTCGGATTCTCCGTTTCT	cFOS reverse
GCTTGTCGATTGCTCAGCTCA	Chrna4 forward
TCCCAGCGCAGTTTGTAGTCA	Chrna4 reverse
CTTTGCTGGTATTCTTGCTGCC	Chrna7 forward
ATCTCAGCCACAAGCAGCATG	Chrna7 reverse
GGAAGCCTGAGGATTTCGACA	Chrnb2 forward
AGACTTCGTACATGCCGTCAGC	Chrnb2 reverse
CCCGACAATGAGCAAACGTAC	Dopamine β-Hydroxylase forward
TTGGAAGACCTCCATGTGGTG	Dopamine β-Hydroxylase reverse
TTAAGGCCGGTGACTGACAGAG	G0S2 forward
TCCCAGACCCCTTAGGTGATCT	G0S2 reverse
GCGACCAAAATTCAGGCTAGC	GAP43 forward
TTCTCCACACCATCAGCAACG	GAP43 reverse
TTGAAGGCAATGACCGCTATG	GluR1 forward
TTTGCCGTCGCTGACAATC	GluR1 reverse
ACCTGGATTCCAAAGGCTACG	GluR2 forward
CCAACAGGCCTTGTTCATTCA	GluR2 reverse

CATTGAGCAGAGAAAGCCGTG	GluR3 forward
GCGTTCCTAATGCTGAGCCTT	GluR3 reverse
AACCTCCCAATGAGTTTGGCA	GluR4 forward
ATACGCCTCCAACAATCCGAC	GluR4 reverse
TGCCTGCAGTGCGATATGAA	Id4 forward
GATAACGTGCTGCAGGATCTCC	Id4 reverse
TTGGCGCAAGATGCTAAAGAG	Itp3R forward
CCCGGAGATTTCATTGATGG	Itp3R reverse
TCGTTAAGCGGCACTTTTTCTC	Ly-6H forward
GCCCCGTTGCACAAATCTT	Ly-6H reverse
CCACACGAACTTACTTCACCCC	Lynx1 forward
AGATGCATGCTTGGAATAGCCA	Lynx1 reverse
CGTAAATTGCACCGTGAACGT	Lynx2 forward
AAGCAATGAGACAGGCTGCTG	Lynx2 reverse
AAACGCAAGATGACCAAGGC	NeuroD2 forward
TCGATCTTGGACAGCTTCTGC	NeuroD2 reverse
TACAGAAAGCTCCTGGAAGGC	Neurofilament heavy chain forward
TTATGTGCGTGGATATGGAGG	Neurofilament heavy chain reverse
TCCTCAGTCAGCCATACCCAAA	NKCC1 forward
ATCCCGAACAACACACGAACC	NKCC1 reverse
TCGAGGATACCAGATGTCCACC	NR1 forward
CCTCTTTGCATGTGCCATCAC	NR1 reverse
TGTTGATGTTCCCGCCTTTG	NR4A1 forward
ATGCGATTCTGCAGCTCTTCC	NR4A1 reverse
TGGCGGAAGACAAATGCAG	NRSF forward
TCCGGATGTGATGCACAAACT	NRSF reverse
TTGGAACCTGGAACCATGGAC	N-Tubulin b3 forward
ATAGTGCCCTTTGGCCCAGTT	N-Tubulin b3 reverse
TGTTGATGTTCCCGCCTTTG	Nur77 forward
ATGCGATTCTGCAGCTCTTCC	Nur77 reverse
TCCCACCTGTTTAGAGCCAGAA	Olig1 forward
CGATGCTCACGGATACGAGAAT	Olig1 reverse
TCAGGAGACACCGTCTTTTGG	SynGAP forward
AACGTAGCCAGCCTTGTCCTT	SynGAP reverse
CAAATGGCCTCCCTCTCATCA	TNFalpha forward
TTGGTGGTTTGCTACGACGTG	TNFalpha reverse
CCTGCGGCACATAAATTTCAC	TrkB-Receptor forward
AACGGATTACCCGTCAGGATC	TrkB-Receptor reverse
CTTCACAATCGAGTTCGGCCT	Tryptophan Hydroxylase 2 forward
CCTTGTCGGAAAGAGCATGCT	Tryptophan Hydroxylase 2 reverse
ACATTTGCCCAGTTCTCCCAG	Tyrosine Hydroxylase forward
CCCAAACTCCACAGTGAACCA	Tyrosine Hydroxylase reverse
AGGCCGAGATGCAATTGATGT	Zif268 forward
TCAGCAGCATCATCTCCTCCA	Zif268 reverse

Supplementary Figure Legends:

Suppl. Figure S1

In-situ hybridization for *Nkcc1* transcripts in the developing hippocampus. (A,C,E,G) Darkfield photomicrographs reveal a decrease of *Nkcc1* transcripts from postnatal day (P) 1 (P1) to P15. Signals in G most likely correspond to glial cells. Hybridization signals appear white in darkfield (sense controls gave no signal). (B,D,F,H) Photomicrographs of Giemsa-stained coronal brain sections at P1, P5, P8 and P15 corresponding to darkfield photomicrographs. (I) Nkcc1 transcript levels in the hippocampus decrease from postnatal day 1 (P1) to P15. Levels were determined by quantitative RT PCR, and normalized to those of hypoxanthine guanine phosphoribosyl transferase (HPRT), and to the WT values at P1 (mean ± SEM, n = 3 animals). (J) Kcc2 transcripts increased during the same period and did not change in *Nkcc1*$^{-/-}$ mice (n = 3 animals per genotype). Scale bar in (H) corresponds to 50 µm for (A-H); pc: pyramidal cell layer; dg: dentate gyrus. Asterisks (**) indicate significance ($p<0.01$, t-test).

Suppl. Figure S2

KO of *Nkcc1* but not of *Ae3* reduces the amplitude of GABA induced Calcium elevations in CA1 neurons at P1. (A,B,C,D) Histogram plots show amplitude distribution of Calcium elevations of WT (black bars) and KO (white bars) slices disrupted for *Nkcc1* (A,C) and *Ae3* (B,D) after GABA (A,B) and glutamate (C,D) application. (Nkcc1: WT 5 mice, 6 recordings, 108 cells; KO 5 mice, 7 recordings, 141 cells; Ae3: WT 3 mice, 7 recordings, 136 cells; KO 3 mice, 5 recordings, 191 cells). Different WT distributions may be due to differences in genetic background of NKCC1 and AE3 mouse lines (see methods/mice).

Suppl. Figure S3A

Detection of spontaneous calcium transients. Representative recordings from P2 and P4 WT and *Nkcc1*$^{-/-}$ slices (also shown in Fig. 2A). Calcium transients that were identified by a mathematical routine (Suppl. Methods) are marked by red

dots. Detection parameters were conservatively chosen to underestimate rather than to overestimate spike rates and synchronous events. Missed events were rare (<10%) while events that were erroneously assigned as calcium transients by the routine were minimized (< 2%). Numbers assigned to each trace correspond to cells in the respective raster plot diagram (Fig. S3B). Scale bars: horizontal 100 s; vertical 0.15 F_{340}/F_{380}.

Suppl. Figure S3B

Raster plot and correlation representation of individual calcium recordings. The fura-2 loaded slice is shown at t=0 in each panel. Individual cells that were analyzed during the subsequent 500 s period are marked by black squares. On the left side of each panel the individual cellular calcium events of these cells, detected by the mathematical routine, are represented by vertical black lines. Each cell is represented by a white bar, bordered by horizontal black lines. The numbers with arrows refer to the traces displayed in Fig. S3A. Cells showing correlated activity are connected by a colored line in the right image of each panel. Color codes right to the image indicate strength of correlated activity by representing the number of synchronous events only for those cell pairs with significant (p<.001) synchronicity. WT cells show correlated activity all over the recorded area, while *Nkcc1*$^{-/-}$ cells do not.

Suppl. Figure S4

KO of *Nkcc1* or *Ae3* reduces the amplitudes of GDPs. Histogram plots show amplitude distribution of GDPs of WT (black bars) and KO (white bars) slices disrupted for *Nkcc1* (A) and *Ae3* (B) (3 animals per genotype; Nkcc1: WT 15 slices, 331 GDP events; KO 19 slices, 115 GDP events; Ae3: WT 11 slices, 384 GDP events; KO 12 slices, 193 GDP events). Different WT distributions may be due to differences in genetic background of NKCC1 and AE3 mouse lines (see methods/mice).

Suppl. Figure S5

GDPs at P10 were unchanged between WT and *Nkcc1*$^{-/-}$ animals. (A) representative traces showing typical GDPs in WT and *Nkcc1*$^{-/-}$ at p10. (B,C,D,E) Quantification of GDPs revealed unchanged amplitude (B), area under curve (C), frequency (D) and histogram plot distribution of the amplitude (E) of WT (black bar) and *Nkcc1*$^{-/-}$ (open bar) animals (3 animals per genotype; WT: 14 slices, *Nkcc1*$^{-/-}$: 17 slices; WT: 107 GDPs, *Nkcc1*$^{-/-}$: 98 GDPs). Scale bars are shown for the respective traces in (A).

Suppl. Figure S6

GABA-induced depolarization in hippocampal CA1 neurons does not depend on AE3 at P1. (A,B) Representative current-voltage traces of hippocampal pyramidal CA1 neurons (P1) from both WT (A) and *Ae3*$^{-/-}$ (B) mice using gramicidin-perforated patch-clamp recordings before and during application of 100 µM GABA. (C) Mean shift in reversal potential (mean ± SEM) upon application of 100 µM GABA in voltage clamp mode does not differ significantly between WT and *Ae3*$^{-/-}$ CA1 neurons (WT: 6 cells from 3 mice, mean ± SEM = 20.2mV ± 4.6mV; *Ae3*$^{-/-}$: 10 cells from 6 mice, mean ± SEM = 23.4mV ± 3.3mV; $p>0.5$, t-test). (D,E,F) Ca^{2+} entry in response to GABA and glutamate in *Ae3*$^{-/-}$ CA1 neurons at P1. (D,E) Typical fura-2 fluorescence traces indicative of intracellular calcium of a single WT (D) and *Ae3*$^{-/-}$ (E) CA1 neuron sequentially exposed to GABA (100 µM) and glutamate (100 µM) for 50 s each. The ratio of fluorescence at 340 nm and 380 nm, which increases with $[Ca^{2+}]_i$, is given. (F) Ca^{2+} responses as indicated by mean (± SEM) changes in fura-2 fluorescence in response to GABA and glutamate in WT (filled bars) and *Ae3*$^{-/-}$ (empty bars) P1 CA1 neurons normalized to WT GABA (WT: 136 cells, 7 recordings, 3 mice, GABA: normalized to 1, Glutamate: mean ± SEM = 3.80 ± 0.14; *Ae3*$^{-/-}$: 191 cells, 5 recordings, 3 mice; GABA: mean ± SEM = 1.01 ± 0.08, Glutamate: mean ± SEM = 3.79 ± 0.17; t-test GABA: $p>0.5$, t-test Glutamate: $p>0.5$).

Suppl. Figure S7

Normal pre- and postsynaptic marker protein levels in the *Nkcc1*$^{-/-}$ hippocampus. (A,B,C,D) Hippocampal protein levels of glutamic acid decarboxylase (GAD) 65/67, gephyrin, the AMPA receptor subunit GluR2 and synaptophysin quantified by Western blots did not differ between genotypes at P1 (A), P5 (B), and P15 (C). Hippocampal KCC2 protein levels (D) were unchanged in *Nkcc1*$^{-/-}$ mice at P1, P5, and P15 (right lane labeled with K2$^{-/-}$ represents KCC2 KO control). Levels of hippocampal GluR1 and GluR1 phosphorylated at serines 831 or 845 did not differ significantly between genotypes at P5 (E) and P15 (F). Phosphorylated CREB (pCREB) and phosphorylated ERK1/2 (pERK1/2[p42/44 MAPK]) did not differ significantly between genotypes at P5 and P15 (G,H) either. (I) The anion exchanger AE3 shows developmental upregulation from P1 to P15 in the hippocampus. No expression level differences could be detected between WT and *Nkcc1*$^{-/-}$ animals. Specificity of the antibody is shown with *Ae3*$^{-/-}$ and WT hippocampal tissue at P6 and P12.

Suppl. Figure S8

Immunofluorescence analysis of selected marker proteins in the hippocampus and cortex of *Nkcc1*$^{-/-}$ mice. (A-H) Double staining for KCC2 (green) and reelin (red) in hippocampus (A,B,E,F) and cortex (C,D,G,H) of P1 WT (A,B,C,D) and *Nkcc1*$^{-/-}$ (E,F,G,H) mice. (I-P) Synaptophysin (green) and microtubule associated protein 2 (MAP-2) (red) in hippocampus (I,J,M,N) and cortex (K,L,O,P) of WT (I,J,K,L) and *Nkcc1*$^{-/-}$ (M,N,O,P) animals at P1. (Q-T) Staining for vGluT1 (green) and calbindin (red) of the projection (mossy fibers) from dendate gyrus cells to CA3 neurons. Squares in (Q) and (S) appear enlarged in (R) and (T). (U-Z) Co-staining of KCC2 with synaptophysin (U,X), of the presynaptic marker synaptosome-associated protein of 25 kDa (SNAP25) with and glutamic acid decarboxylase GAD65-67 (V,Y) and staining for the $GABA_A$-receptor subunit α3 (W,Z) in CA1 stratum radiatum of WT (U,V,W) and *Nkcc1*$^{-/-}$ (X,Y,Z) mice. Nuclei stained by TOTO-3 are shown in blue. Scale bars: (A) 100 µm (A-P without J,N), (J) 23 µm for (J,N), (Q) 100 µm for (Q,S), (R) 21 µm, (T) 15 µm, (U) 35 µm for

(U,V,X,Y) and in (W), 20 µm for (W,Z). No difference between WT and *Nkcc1*$^{-/-}$ sections is seen in any of the panels.

Suppl. Figure S9

Glutamatergic neurotransmission in P15 brain slices. (A) Field excitatory postsynaptic potentials (fEPSP) of WT and *Nkcc1*$^{-/-}$ slices in CA1 stratum radiatum show intact glutamatergic transmission (mean ± SEM, WT: 6 slices, 3 mice; KO: 7 slices, 3 mice; t-test: $p>0.1$). Representative sample traces for the given fiber volley amplitudes (0.2, 0.4, 0.6, 0.8 mV) are displayed above. Stimulation artifacts were omitted for clarity. (B) Paired pulse facilitation (PPF) in the CA1 stratum radiatum at inter stimulus intervals (ISI) of 40 ms and 100 ms, respectively (mean ± SEM, WT: 6 slices, 3 mice; KO: 7 slices, 3 mice; t-test: $p>0.1$). Representative sample traces are shown above. Stimulation artifacts were omitted for clarity. Scale bars: (A): horizontal 10 ms, vertical 0.4 mV; (B): horizontal 20 ms, vertical 0.4 mV. No significant difference between WT and *Nkcc1*$^{-/-}$ transmission is detectable in either test paradigm.

Suppl. Figure S10

Quantification of expression levels of selected genes relevant for transcription, development, and neurotransmission as assessed by qRT-PCR at P1, P5 and P15. The percentage of WT transcription (± SEM) is given. Quantification of at least 3 animals per genotype per time point. No significant differences were observed.

Suppl. Figure S11

Normal localization of GluR4 in interneurons of the hippocampus. (A,B,C,D) GluR4 (green) is localized to GAD (red) positive GABAergic interneurons in CA1 (A,B) and dentate gyrus (C,D) of P15 WT (A,C) and *Nkcc1*$^{-/-}$ mice. Not all GABAergic interneurons express GluR4 (white arrows). (E,F,G,H) The overall quantity and distribution of GluR4 (green) is similar between WT (E,G) and

Nkcc1$^{-/-}$ (F,H) hippocampus. Calbindin (red) stains the mossy fibers and outlines the hippocampal CA3 region. Scale bar: in (A) for (A-D) 500µm; for (E-H) 125µm.

Suppl. Figure S12

Comparative expression profiling of the P5 hippocampus. (A) Genes upregulated in the P5 *Nkcc1*$^{-/-}$ hippocampus. (B) Genes downregulated in the P5 *Nkcc1*$^{-/-}$ hippocampus. Affymetrix probe set numbers, ID's for the corresponding RefSeq, a short gene description and the calculated fold change are displayed. Genes underlined in red were further assessed by qRT-PCR.

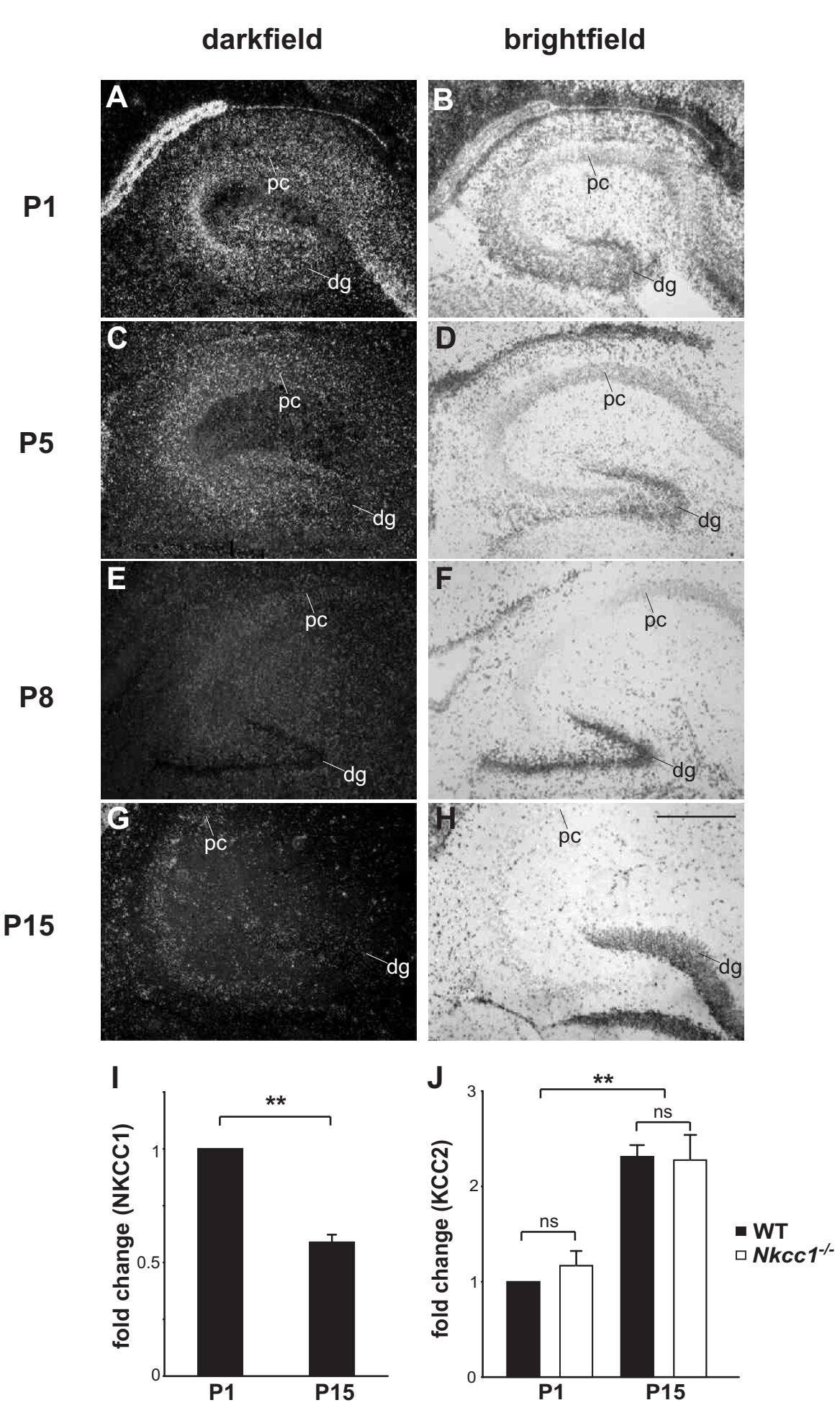

Pfeffer et al. Supplementary Figure S1

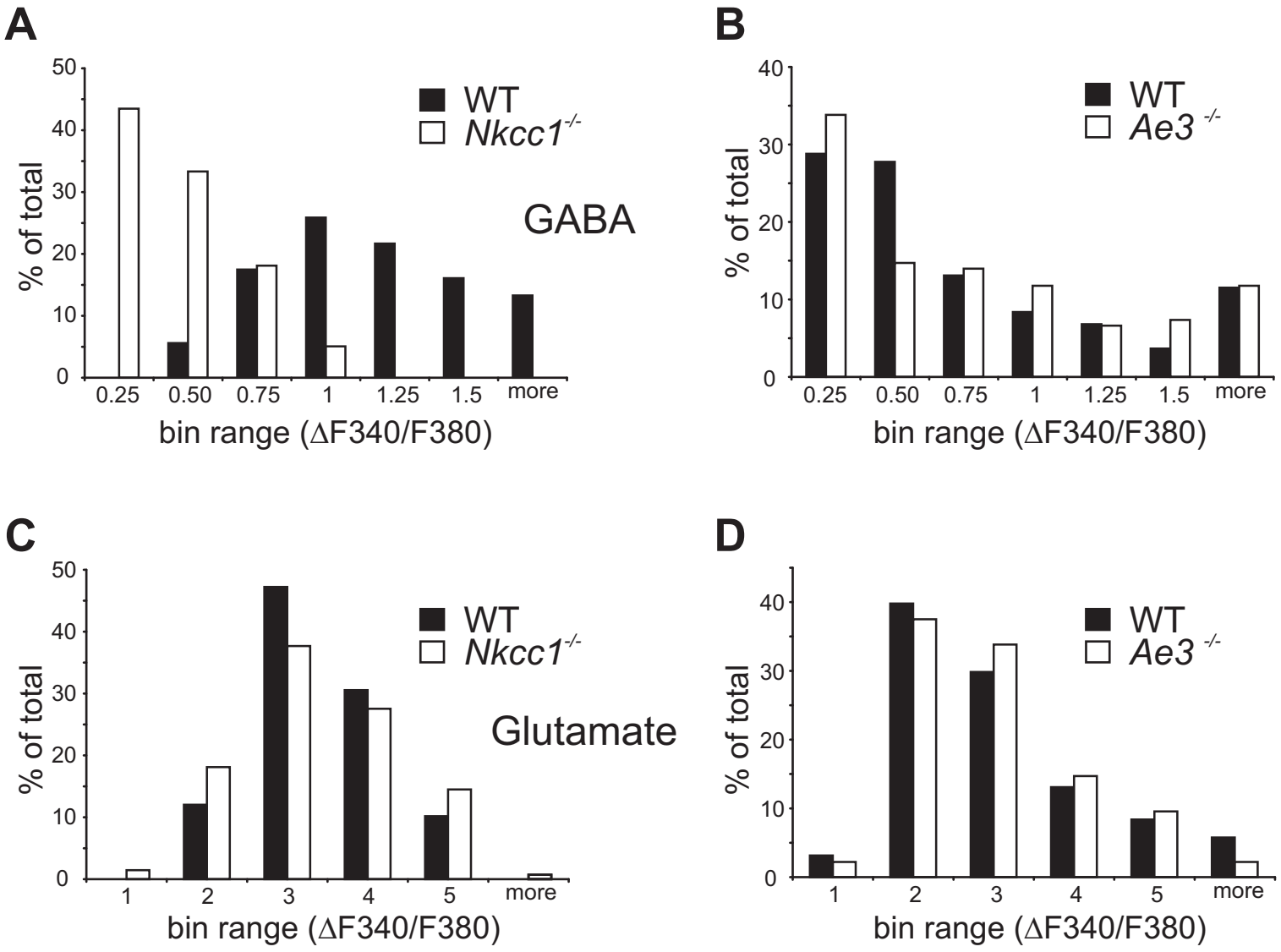

Pfeffer et al. Supplementary Figure S2

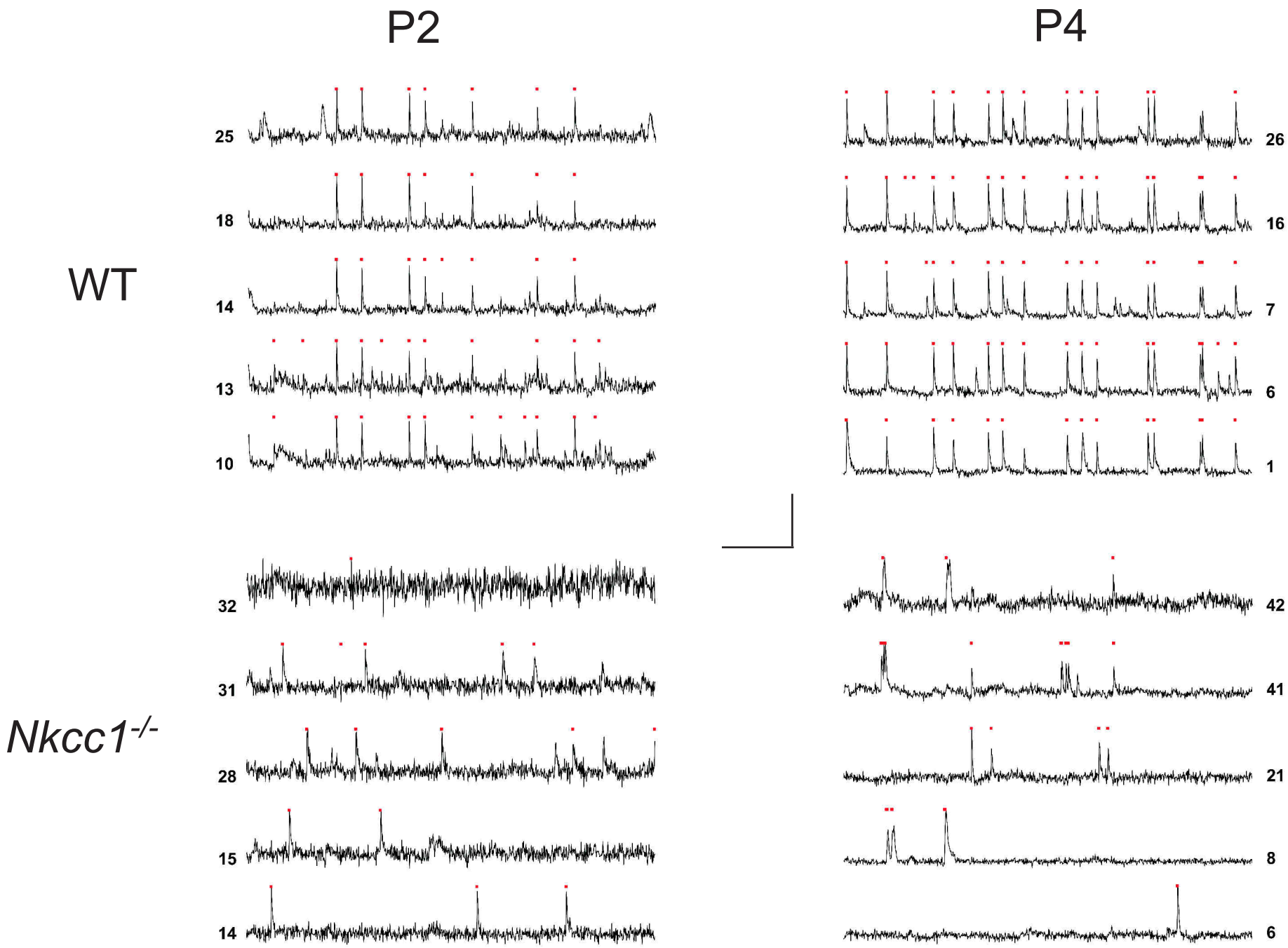

Pfeffer et al. Supplementary Figure S3A

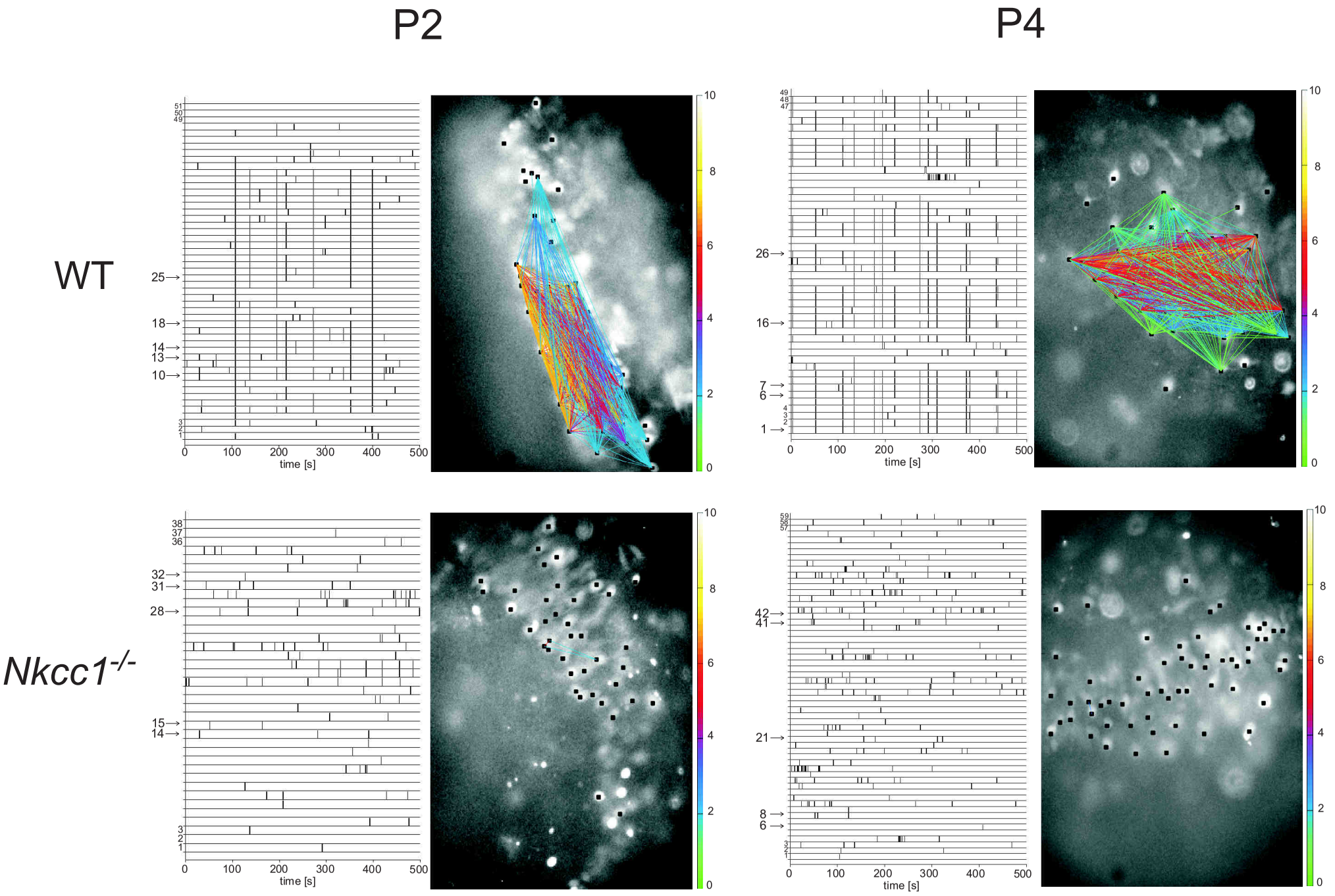

Pfeffer et al. Supplementary Figure S3B

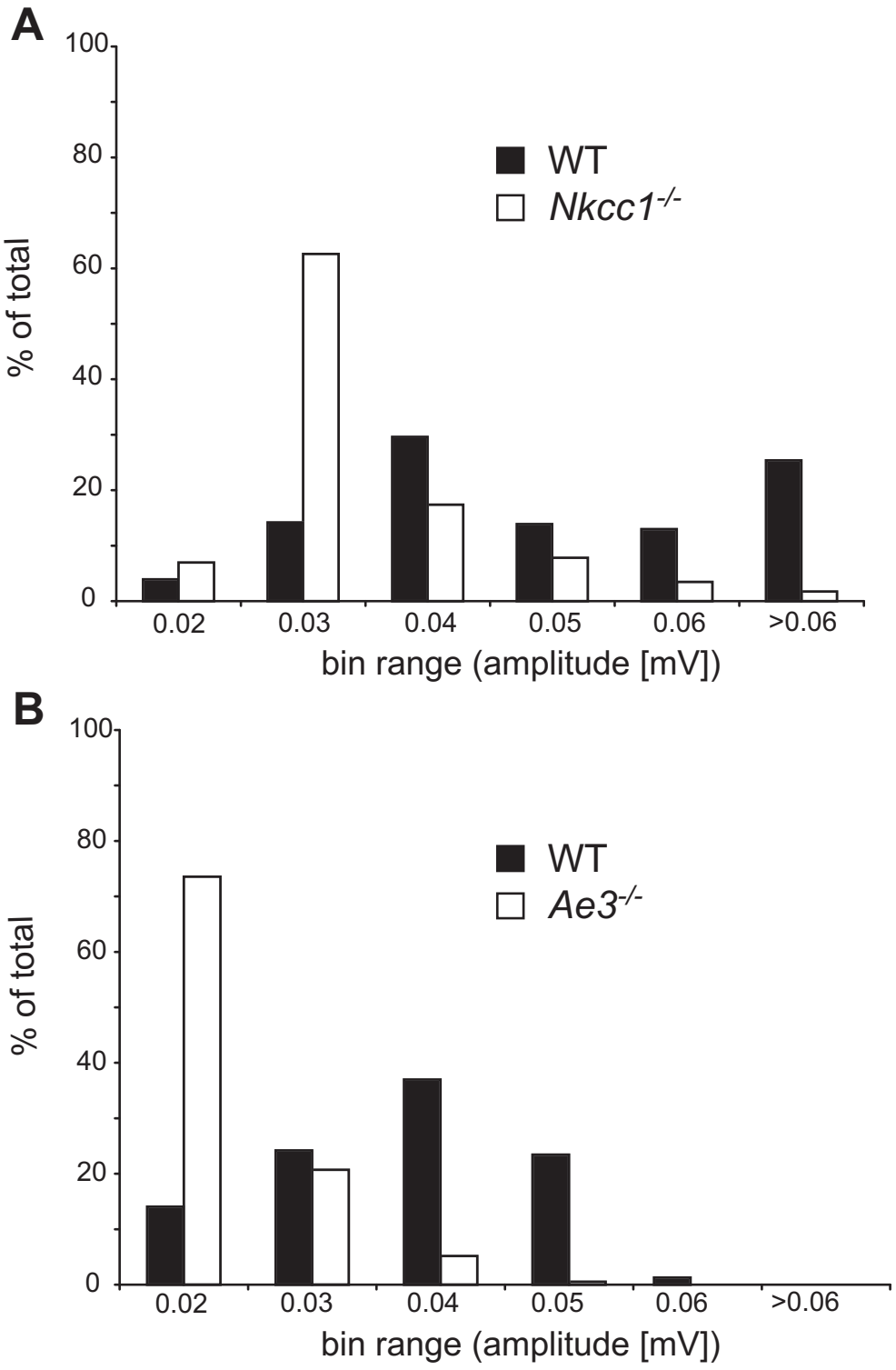

Pfeffer et al. Supplementary Figure S4

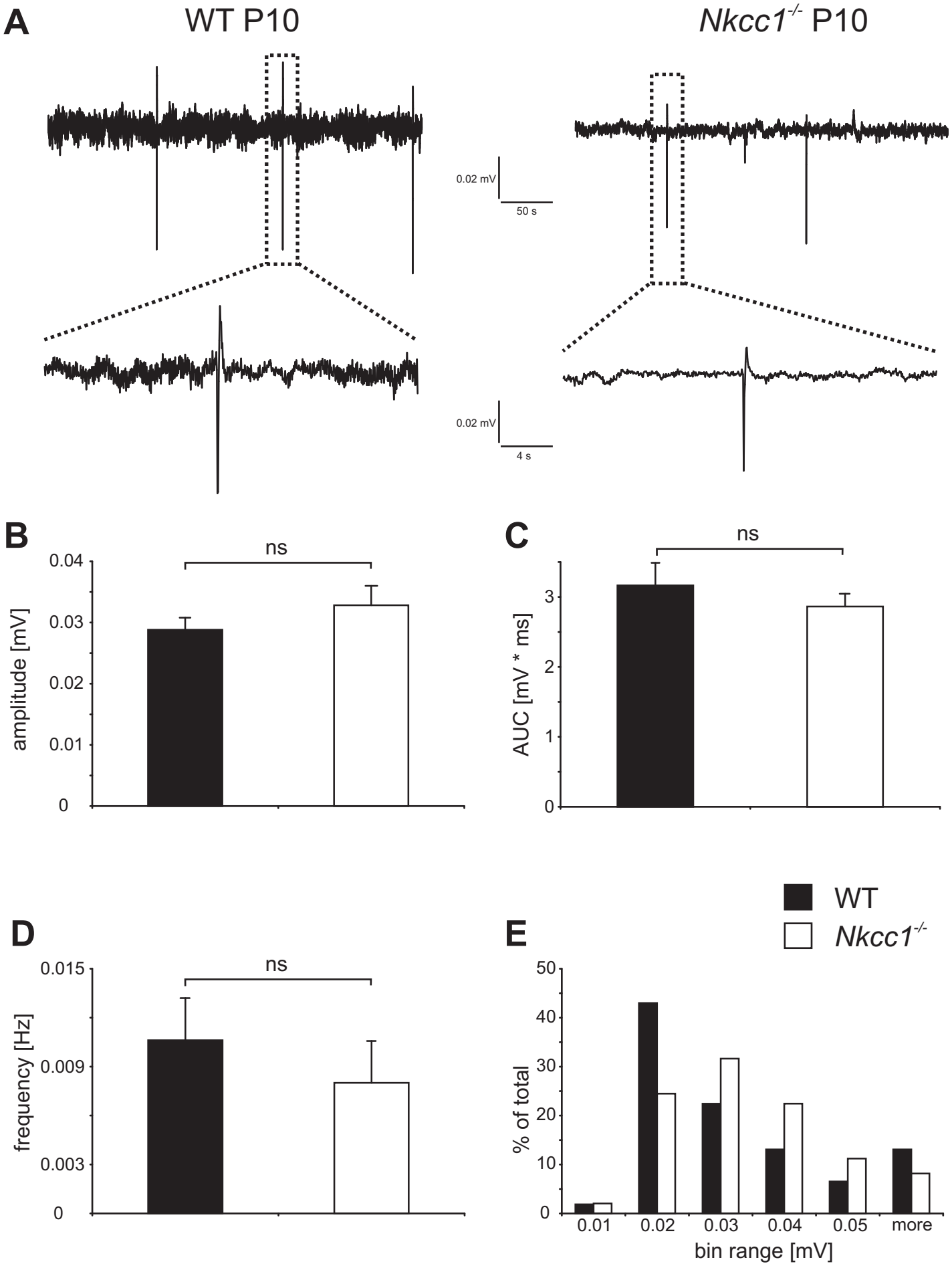

Pfeffer et al. Supplementary Figure S5

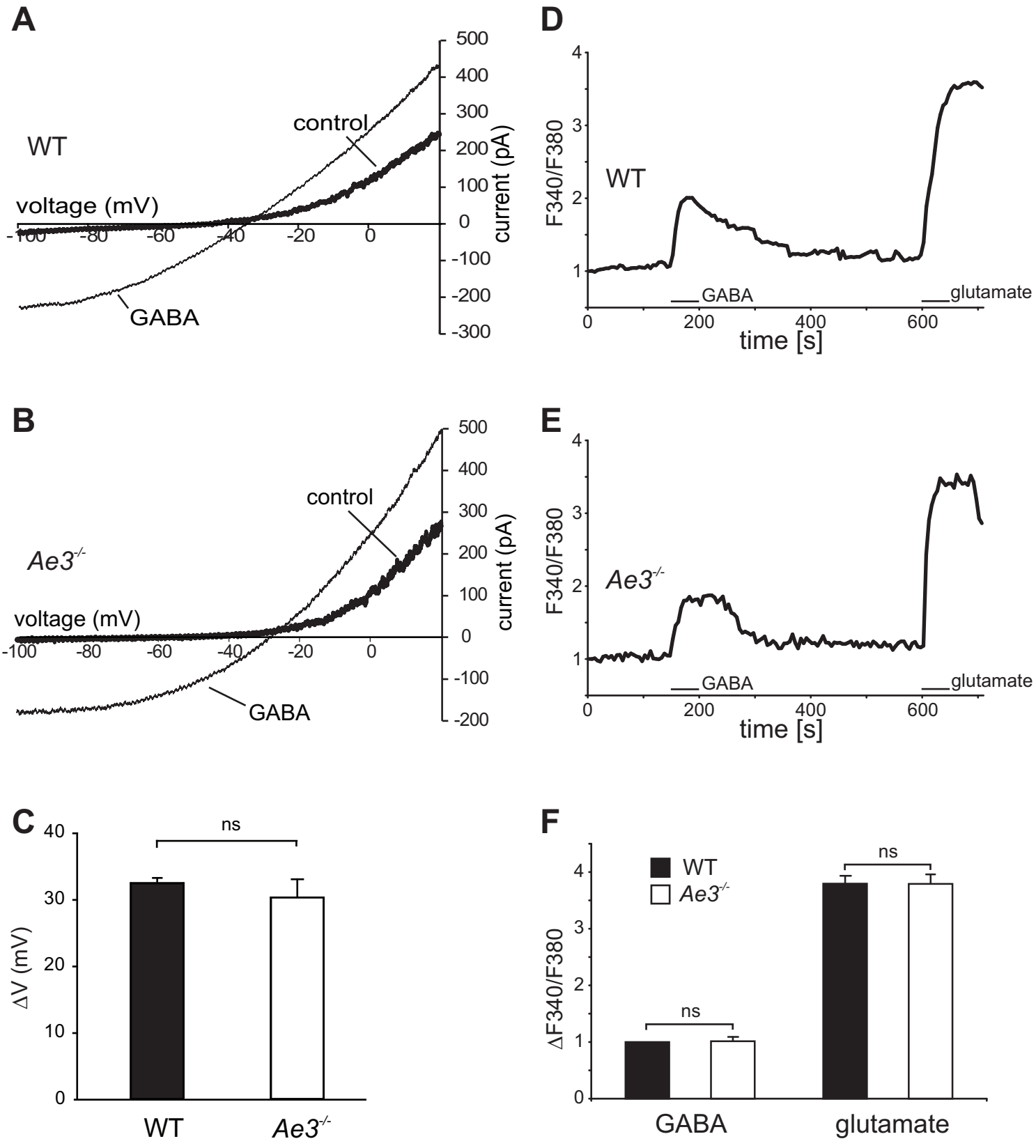

Pfeffer et al. Supplementary Figure S6

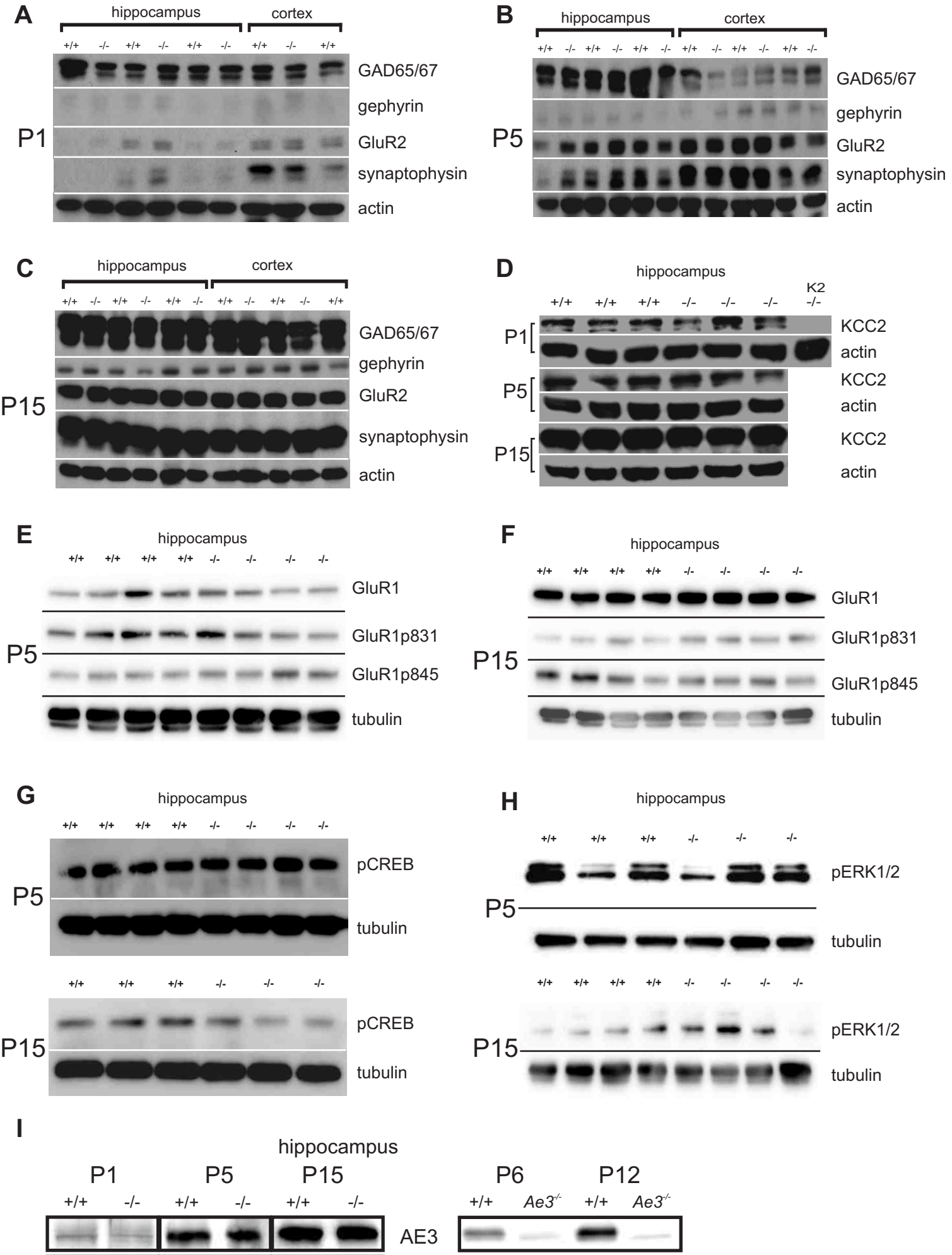

Pfeffer et al. Suppl. Figure S7

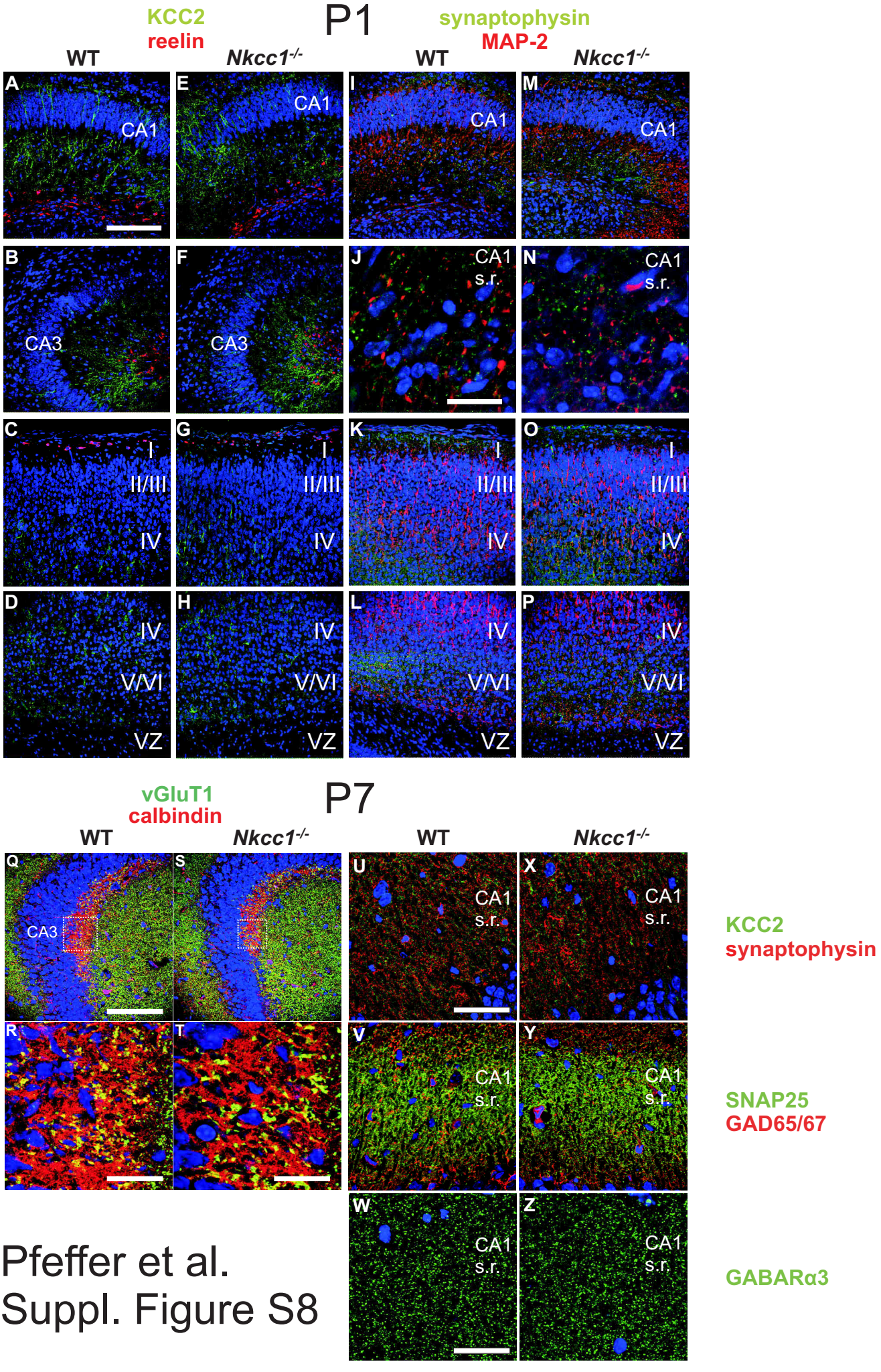

Pfeffer et al.
Suppl. Figure S8

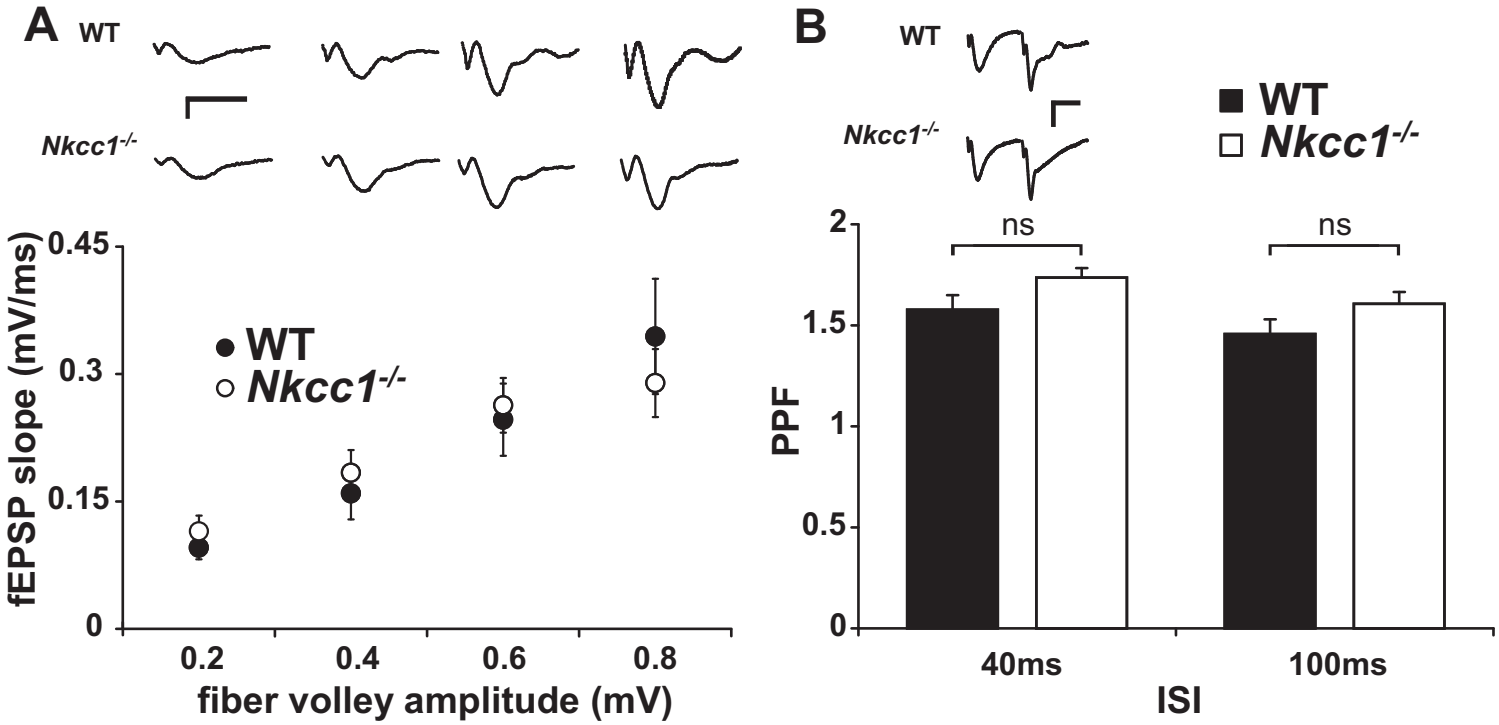

Pfeffer et al. Supplementary Figure S9

qRT-PCR quantification of selected genes in *Nkcc1*$^{-/-}$ vs WT:

Gene	P1 KO vs. WT (%)	SEM(%)	P5 KO vs. WT (%)	SEM(%)	P15 KO vs. WT (%)	SEM(%)
Na-K-2Cl Cotransporter 1 (NKCC1)	0.1	0.0	0.3	0.1	1.5	0.4
Activity-regulated gene 3.1 protein homolog (Arg3.1/Arc)	125.1	48.8	96.2	16.2	100.4	15.1
V-Fos FBJ Murine Osteosarcoma Viral Oncogene Homolog (cFos)	75.1	26.5	108.8	6.4	90.1	8.6
Early Growth Response 1 (Egr1,Zif268)	91.8	19.9	102.8	9.1	97.4	21.0
Dopamine b-Hydroxylase (DbH)	101.8	15.9	119.5	28.6	108.0	60.7
Tryptophan Hydroxylase 2 (TrpH2)	78.1	13.0	78.2	2.7	78.8	11.4
Tyrosine Hydroxylase (TH)	135.4	24.4	72.5	18.4	109.5	38.6
Synaptic RAS-GTPase-Activating Potein 1 (SynGap)	82.7	10.6	108.9	9.8	93.5	12.0
Nuclear Receptor Subfamily 4, A, 1 (NR4A1)	101.3	14.9	95.2	10.9	87.4	23.0
Growth Associated Protein 43 (GAP43)	110.0	11.5	90.2	9.2	101.1	2.9
Neurogenic Differentiation 2 (NeuroD2)	100.6	1.7	101.7	9.4	83.6	1.8
Neuron Restrictive Silencing Factor (NRSF)	92.5	4.5	90.6	11.5	137.7	2.7
N-Tubulin	84.6	11.0	78.1	6.0	94.8	3.3
Tumor Necrosis Factor alpha (TNFalpha)	110.9	23.2	97.8	24.4	113.8	4.5
Brain Derived Neurotrophic Factor (BDNF) exon4	96.5	27.7	118.7	31.9	100.4	31.9
Tyrosine Kinase Receptor B (TrkB)	82.9	11.3	95.5	6.7	77.8	10.8
Inositol 1,4,5-TriPhosphat Receptor 3 (Itp3R)	94.5	19.3	103.4	32.6	106.7	11.0
Glutamate Receptor subunit 1 (GluR1)	88.2	32.0	84.7	20.4	120.3	7.6
Glutamate Receptor subunit 2 (GluR2)	101.4	19.7	84.9	12.7	105.1	32.7
Glutamate Receptor subunit 3 (GluR3)	106.7	24.4	76.1	21.3	129.5	21.8
Glutamate Receptor subunit 4 (GluR4)	107.6	11.2	88.1	4.4	110.4	19.9
NMDA Rezeptor subunit 1 (NR1)	127.5	29.3	97.5	24.6	73.0	37.3
Anion Exchanger 3 (AE3)	69.9	3.5	124.7	20.4	98.0	24.8

Pfeffer et al. Supplementary Figure S10

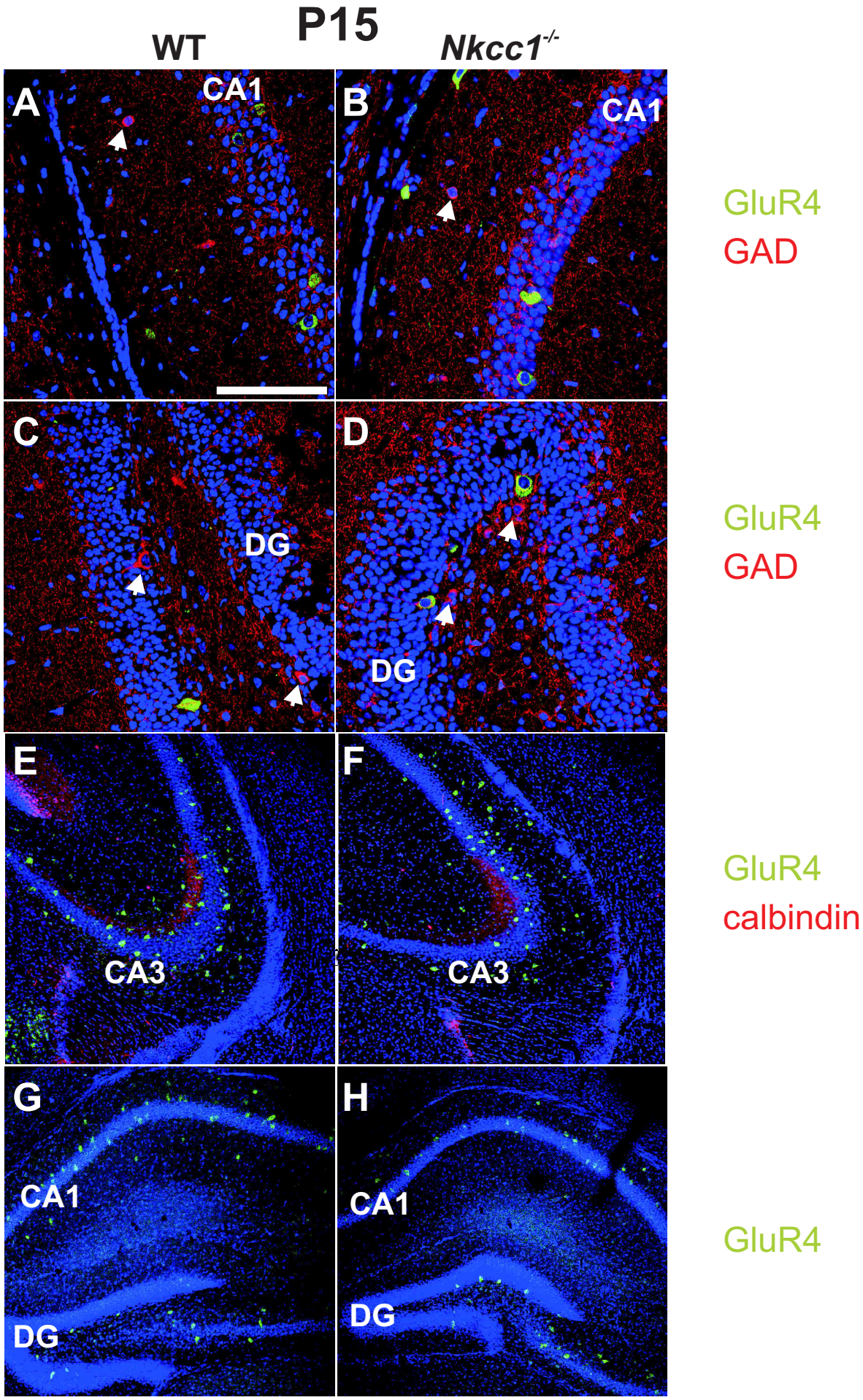

Pfeffer et al. Supplementary Figure S11

A

genes upregulated in *Nkcc1*$^{-/-}$ on gene chips at P5:

Probesets	RefSeq Transcript ID	Fold Change	Gene Title
1450928_at	NM_031166	1.54	inhibitor of DNA binding 4
1423259_at	NM_031166	1.53	inhibitor of DNA binding 4
1455886_at	NM_007619	1.46	Casitas B-lineage lymphoma
1452671_s_at	NM_027400	1.40	lectin, mannose-binding, 1
1450042_at	NM_007492	1.40	aristaless related homeobox gene (Drosophila)
1428282_at	NM_178337	1.37	tubulin-specific chaperone e
1427902_at	NM_175229	1.37	serine/arginine repetitive matrix 2
1423760_at	NM_001039150	1.37	CD44 antigen
1426968_a_at	NM_133832	1.36	retinol dehydrogenase 10 (all-trans)
1428467_at	NM_001003898	1.35	TAR DNA binding protein
1452114_s_at	NM_010518	1.35	insulin-like growth factor binding protein 5
1448199_at	NM_133971	1.35	ankyrin repeat domain 10
1420836_at	NM_026232	1.35	solute carrier family 25, member 30
1419286_s_at	NM_009879	1.35	intraflagellar transport 81 homolog (Chlamydomonas)
1452036_a_at	NM_011605	1.34	thymopoietin
1427084_a_at	NM_024275	1.33	mitogen-activated protein kinase kinase kinase kinase 5
1416700_at	NM_028810	1.33	Rho family GTPase 3
1424135_at	NM_026274	1.33	ring finger and SPRY domain containing 1
1451289_at	NM_019978	1.32	doublecortin and calcium/calmodulin-dependent protein kinase-like 1
1416814_at	NM_011585	1.32	cytotoxic granule-associated RNA binding protein 1
1426985_s_at	NM_176836	1.30	RIKEN cDNA 2810485I05 gene
1451980_at	NM_145398	1.30	CAS1 domain containing 1
1431921_a_at	NM_009282	1.30	stromal antigen 1

B

genes downregulated in *Nkcc1*$^{-/-}$ on gene chips at P5:

Probesets	RefSeq Transcript ID	Fold Change	Gene Title
1421653_a_at	XM_001004859	0.52	immunoglobulin heavy chain (J558 family)
1433809_at	NM_007840	0.61	DEAD (Asp-Glu-Ala-Asp) box polypeptide 5
1418636_at	NM_012051	0.64	ets variant gene 3
1425902_a_at	NM_019408	0.65	nuclear factor of kappa light polypeptide gene enhancer in B-cells 2, p49/p100
1422904_at	NM_018881	0.65	flavin containing monooxygenase 2
1455115_a_at	NM_177638	0.65	crumbs homolog 3 (Drosophila)
1425866_a_at	NM_148927	0.65	pleckstrin homology domain containing, family A member 4
1434137_x_at	NM_026918	0.65	RIKEN cDNA 1810010M01 gene
1422377_at	NM_053227	0.65	vomeronasal 1 receptor, B4
1427576_at	---	0.68	immunoglobulin kappa chain variable 28 (V28)
1424847_at	NM_010904	0.70	neurofilament, heavy polypeptide
1427734_a_at	XM_001002206	0.70	Down syndrome cell adhesion molecule-like 1
1460167_at	NM_138600	0.70	aldehyde dehydrogenase family 7, member A1
1422403_at	NM_008334	0.70	interferon alpha
1419383_at	NM_009115	0.72	S100 protein, beta polypeptide, neural
1450196_s_at	NM_030678	0.72	glycogen synthase 1, muscle
1437686_x_at	NM_009986	0.73	cut-like 1 (Drosophila)
1449499_at	NM_010455	0.73	homeo box A7
1431227_at	NM_027149	0.73	RIKEN cDNA 2310040A13 gene
1434932_at	NM_001024837	0.73	adenosine deaminase, RNA-specific, B1
1420170_at	NM_022410	0.73	myosin, heavy polypeptide 9, non-muscle
1448700_at	NM_008059	0.73	G0/G1 switch gene 2
1455910_at	NM_027910	0.73	kelch domain containing 3
1427824_at	---	0.73	---
1420663_at	NM_009565	0.73	Vzinc finger and BTB domain containing 7B
1448041_at	NM_011277	0.74	ring finger protein 2
1421500_at	NM_009293	0.74	steroid sulfatase
1419426_s_at	NM_011124	0.74	chemokine (C-C motif) ligand 21
1421453_at	NM_021566	0.74	junctophilin 2
1418411_at	NM_015821	0.74	F-box and leucine-rich repeat protein 8
1426970_a_at	NM_023738	0.74	ubiquitin-activating enzyme E1-like
1452528_a_at	NM_008699	0.74	NK2 transcription factor related, locus 3 (Drosophila)
1448043_x_at	NM_011277	0.75	ring finger protein 2
1424651_at	NM_144932	0.75	cDNA sequence BC021611
1453389_a_at	NM_018825	0.75	SH2B adaptor protein 2
1422404_x_at	NM_008334	0.75	interferon alpha
1421167_at	NM_015804	0.75	ATPase, class VI, type 11A
1417283_at	NM_011838	0.75	Ly6/neurotoxin 1

Pfeffer et al. Supplementary Figure S12